

# Robust voltage regulation of boost converters in DC microgrids\*

Michele Cucuzzella<sup>1</sup>, Riccardo Lazzari<sup>2</sup>, Sebastian Trip<sup>1</sup>, Carlo Sandroni<sup>2</sup> and Antonella Ferrara<sup>3</sup>

**Abstract**—This paper deals with the design of a robust decentralized control scheme for voltage regulation in boost-based DC microgrids. The proposed solution consists of the design of a suitable manifold on which voltage regulation is achieved, even in presence of unknown load demand and modelling uncertainties. A second order sliding mode control is used to constrain the state of the microgrid to this manifold by generating continuous control inputs that can be used as duty cycles of the power converters. The proposed control scheme has been validated through experiments on a real DC microgrid.

## I. INTRODUCTION

Nowadays, due to economical, technological and environmental reasons, the most relevant challenge in power grids deals with the transition from the traditional power generation and transmission systems towards the large scale introduction of smaller Distributed Generation units (DGus) [1]. Moreover, due to the ever-increasing energy demand and the public concern about global warming and climate change, much effort has been focused on the diffusion of environmentally friendly Renewable Energy Sources (RES) [2]. In this context, in order to integrate different types of RES, the so-called *microgrids* have been proposed as a new concept of electric power systems [3]. Microgrids are electrical distribution networks, composed of clusters of DGus, loads, energy storage systems and energy conversion devices interconnected through power distribution lines [4].

Since electrical Alternating Current (AC) has been widely used in most industrial, commercial and residential applications, AC microgrids have attracted the attention of many control system researchers [5]–[10]. However, several advantages of DC microgrids with respect to AC microgrids are well known [11]. The most important advantage relies on the natural interface of many types of RES, energy

storage systems and loads with DC network, through DC-DC converters. For this reason, lossy conversion stages are reduced and consequently DC microgrids are more efficient than AC microgrids. Furthermore, control systems for a DC microgrid are less complex than the ones required for an AC microgrid, where several issues such as synchronization, frequency regulation, reactive power flows, harmonics and unbalanced loads need to be addressed.

Two main control objectives in DC microgrids are voltage regulation and current or power sharing. Typically, both objectives are simultaneously achieved by designing hierarchical control schemes. In the literature, these control problems have been addressed by different approaches [12]–[18]. All these works deal with DC-DC buck converters or do not take into account the model of the power converter. However, considering that many battery-powered applications (e.g. electric vehicles and lighting systems) often stack cells in series to increase the voltage level, DC-DC *boost* converters can be used in order to achieve higher voltage and reduce the number of cells. In this paper a Sliding Mode (SM) control scheme is proposed to regulate the voltage of boost converters within a DC microgrid, which is experimentally shown to be compatible with additional secondary controllers.

The sliding mode control methodology [19] is well known for its robustness properties and, belonging to the class of Variable Structure Control systems, has been extensively applied to power electronics, since it is perfectly adequate to control the inherently variable structure nature of power converters. In this paper we propose robust decentralized primary controllers, relying on a Second Order SM (SOSM) control methodology, capable of dealing with unknown load and input voltage dynamics, as well as uncertain model parameters, without requiring the use of observers. Due to its decentralized and robust nature, the design of each local controller does not depend on the knowledge of the whole microgrid, making the control synthesis simple and the control scheme scalable. The proposed controllers generate continuous inputs that can be used as duty cycles, in order to achieve constant switching frequency. The proposed control scheme has been validated through experimental tests on a real DC microgrid test facility at Ricerca sul Sistema Energetico (RSE), in Milan, Italy [20], showing good closed-loop performances.

## II. DC MICROGRID MODEL

The considered low-voltage DC network is represented by a connected and undirected graph  $\mathcal{G} = (\mathcal{V}, \mathcal{E})$ , where the nodes  $\mathcal{V} = \{1, \dots, n\}$ , represent the DGus and the edges  $\mathcal{E} =$

\*This work has been financed by the Research Fund for the Italian Electrical System under the Contract Agreement between RSE S.p.A. and the Ministry of Economic Development - General Directorate for Nuclear Energy, Renewable Energy and Energy Efficiency in compliance with the Decree of March 8, 2006. This work is part of the EU Projects MatchIT (project number 82203), ITEAM (project number 675999), and is part of the research programme ENBARK+ (project number 408.urs+.16.005), which is (partly) financed by the Netherlands Organisation for Scientific Research (NWO).

<sup>1</sup>M. Cucuzzella and S. Trip are with Jan C. Willems Center for Systems and Control, ENTEG, Faculty of Science and Engineering, University of Groningen, Nijenborgh 4, 9747 AG Groningen, the Netherlands m.cucuzzella@rug.nl, s.trip@rug.nl

<sup>2</sup>R. Lazzari and C. Sandroni are with the Department of Power Generation Technologies and Materials, RSE S.p.A., via Rubattino Raffaele 54, 20134 Milan, Italy Riccardo.Lazzari@rse-web.it, Carlo.Sandroni@rse-web.it

<sup>3</sup>A. Ferrara is with Dipartimento di Ingegneria Industriale e dell'Informazione, University of Pavia, via Ferrata 5, 27100 Pavia, Italy antonella.ferrara@unipv.it

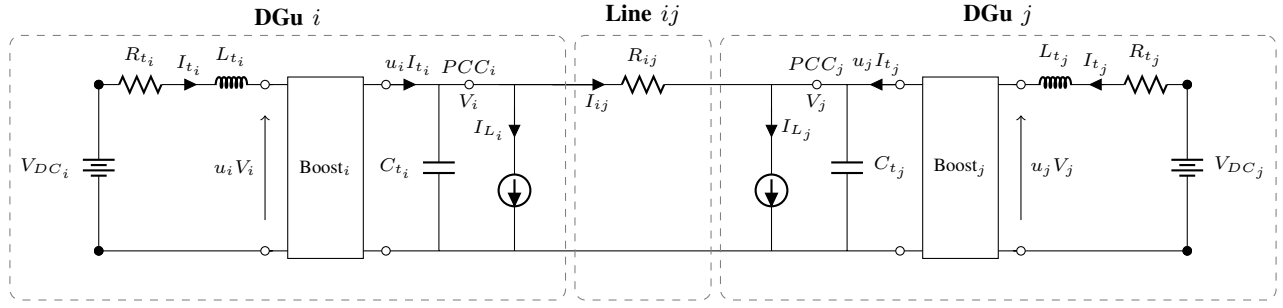


Fig. 1. The considered electrical scheme of a typical boost-based DC microgrid composed of two DGUs.

TABLE I  
DESCRIPTION OF THE USED SYMBOLS

$I_{t_i}$	Inductor current
$V_i$	Boost output voltage
$I_{ij}$	Exchanged current
$R_{t_i}$	Filter resistance
$L_{t_i}$	Filter inductance
$C_{t_i}$	Shunt capacitor
$R_{ij}$	Line resistance
$u_i$	Control input
$V_{DC_i}$	Voltage source
$I_{L_i}$	Unknown current demand

$\{1, \dots, m\}$ , represent the distribution lines interconnecting the DGUs. Consider the scheme reported in Fig. 1. By applying the Kirchhoff's laws, and by using an average switching method, the governing dynamic equations\* of the  $i$ -th node are the following:

$$\begin{aligned} L_{t_i} \dot{I}_{t_i} &= -R_{t_i} I_{t_i} - u_i V_i + V_{DC_i} \\ C_{t_i} \dot{V}_i &= u_i I_{t_i} - I_{L_i} - \sum_{j \in \mathcal{N}_i} I_{ij}, \end{aligned} \quad (1)$$

where  $\mathcal{N}_i$  is the set of nodes (i.e., DGUs) connected to the  $i$ -th DGU by distribution lines, while  $u_i = 1 - \delta_i$  is the control input and  $\delta_i$  is the duty cycle ( $0 \leq \delta_i \leq 1$ ). Exploiting the Quasi Stationary Line (QSL) approximation<sup>†</sup> of the power lines [21], for each  $j \in \mathcal{N}_i$ , one has

$$I_{ij} = \frac{1}{R_{ij}} (V_i - V_j). \quad (2)$$

The symbols used in (1) and (2) are described in Table I.

**Remark 1 (Kron reduction)** In (1), the load currents are located only at the Point of Common Coupling (PCC) of each DGU. However, by using the Kron reduction method, it is possible to map arbitrary interconnections of DGUs and loads, into a reduced network with only local loads [22].

The network topology can be represented by its corresponding incidence matrix  $\mathcal{B} \in \mathbb{R}^{n \times m}$ . The ends of edge  $k$  are

\*For the sake of simplicity, the dependence of all the variables on time  $t$  is omitted throughout the paper.

<sup>†</sup>The QSL approximation is valid for low-voltage networks, where the lines are predominantly resistive and the inductance negligible.

arbitrarily labeled with a  $+$  and a  $-$ . More precisely, one has that

$$\mathcal{B}_{ik} = \begin{cases} +1 & \text{if } i \text{ is the positive end of } k \\ -1 & \text{if } i \text{ is the negative end of } k \\ 0 & \text{otherwise.} \end{cases}$$

Let ' $\circ$ ' denote the Hadamard product, i.e., given  $p, q \in \mathbb{R}^n$ , then  $(p \circ q) \in \mathbb{R}^n$  with  $(p \circ q)_i = p_i q_i$  for all  $i \in \mathcal{V}$ . After substituting (2) in (1), the overall microgrid system can be written compactly for all nodes  $i \in \mathcal{V}$  as

$$\begin{aligned} L_t \dot{I}_t &= -R_t I_t - u \circ V + V_{DC} \\ C_t \dot{V} &= u \circ I_t - \mathcal{B} R^{-1} \mathcal{B}^T V - I_L, \end{aligned} \quad (3)$$

where  $I_t, V, V_{DC}, I_L, u \in \mathbb{R}^n$ , and  $C_t, L_t, R_t, R$  are positive definite diagonal matrices of appropriate dimensions.

### III. PROBLEM FORMULATION

In order to permit the controller design in the next sections, the following assumption is introduced:

**Assumption 1 (Available information)** The state variables  $I_{t_i}$  and  $V_i$  are locally available only at the  $i$ -th DGU. The network parameters  $R_{t_i}, R_i, L_{t_i}, C_{t_i}$ , the current disturbance  $I_{L_i}$ , and the voltage source  $V_{DC_i}$  are constant, unknown but bounded, with bounds a-priori known.

**Remark 2 (Decentralized control)** Since, according to Assumption 1, the values of  $I_{t_i}$  and  $V_i$  are available only at the  $i$ -th DGU, the control scheme to regulate the voltages needs to be fully decentralized.

**Remark 3 (Varying uncertainty)** The uncertain terms are required to be constant (Assumption 1) only to allow for a steady state solution and to theoretically analyze its stability.

Note that given a constant current disturbance  $I_L$ , and a constant voltage source  $V_{DC}$ , there exist a constant control input  $\bar{u}$  and a steady state solution  $(\bar{I}_t, \bar{V})$  to system (3) that satisfy

$$\begin{aligned} \bar{I}_t &= R_t^{-1} (-\bar{u} \circ \bar{V} + V_{DC}) \\ \mathcal{B} R^{-1} \mathcal{B}^T \bar{V} &= \bar{u} \circ \bar{I}_t - I_L. \end{aligned} \quad (4)$$

The second line of (4) implies<sup>‡</sup> that at the steady state the total generated current  $\mathbf{1}_n^T(\bar{u} \circ \bar{I}_t)$  is equal to the total current demand  $\mathbf{1}_n^T I_L$ . To formulate the control objective, aiming at voltage regulation, it is assumed that for every DGU, there exists a desired reference voltage  $V_i^*$ .

**Assumption 2 (Desired voltage)** *There exists a constant reference voltage  $V_i^*$  at the PCC, for all  $i \in \mathcal{V}$ .*

The objective is then formulated as follows: Given system (3), and given a  $V^* = [V_1^*, \dots, V_n^*]^T$ , we aim at designing a fully decentralized control scheme capable of guaranteeing voltage regulation, i.e.

### Objective 1 (Voltage regulation)

$$\lim_{t \rightarrow \infty} V(t) = \bar{V} = V^*. \quad (5)$$

## IV. THE PROPOSED SOLUTION

In this section a fully decentralized SOSM control scheme is proposed in order to achieve Objective 1, providing a continuous control input. As a first step, system (3) is augmented with additional state variables  $\theta_i$  for all  $i \in \mathcal{V}$ , resulting in:

$$\begin{aligned} L_t \dot{I}_t &= -R_t I_t - u \circ V + V_{DC} \\ C_t \dot{V} &= u \circ I_t - \mathcal{B} R^{-1} \mathcal{B}^T V - I_L \\ \dot{\theta} &= -(V - V^*). \end{aligned} \quad (6)$$

The additional state  $\theta$  will be coupled to the control input  $u$  via the proposed control scheme, and its dynamics provide a form of integral action that is helpful to obtain the desired voltage regulation.

Now, to facilitate the discussion, some definitions are recalled that are essential to SM control. To this end, consider system

$$\dot{x} = \zeta(x, u), \quad (7)$$

with  $x \in \mathbb{R}^n$ ,  $u \in \mathbb{R}^m$ .

**Definition 1 (Sliding function)** *The sliding function  $\sigma(x) : \mathbb{R}^n \rightarrow \mathbb{R}^m$  is a sufficiently smooth output function of (7).*

**Definition 2 (Sliding manifold)** *The  $r$ -sliding manifold<sup>§</sup> is given by*

$$\{x \in \mathbb{R}^n, u \in \mathbb{R}^m : \sigma = L_\zeta \sigma = \dots = L_\zeta^{(r-1)} \sigma = \mathbf{0}\}, \quad (8)$$

where  $L_\zeta^{(r-1)} \sigma$  is the  $(r-1)$ -th order Lie derivative of  $\sigma$  along the vector field  $\zeta$ . With a slight abuse of notation, also  $L_\zeta \sigma = \dot{\sigma}$ , and  $L_\zeta^{(2)} \sigma = \ddot{\sigma}$  are used in the remainder.

**Definition 3 (Sliding mode order)** *An  $r$ -order sliding mode is enforced from  $t = T_r \geq 0$ , when, starting from an initial condition, the state of (7) reaches the  $r$ -sliding*

<sup>‡</sup>The incidence matrix  $\mathcal{B}$  satisfies  $\mathbf{1}_n^T \mathcal{B} = \mathbf{0}$ , where  $\mathbf{1}_n \in \mathbb{R}^n$  is the vector consisting of all ones.

<sup>§</sup>For the sake of simplicity, the order  $r$  of the sliding manifold is omitted in the remainder of this paper.

manifold, and remains there for all  $t \geq T_r$ . The order of a sliding mode controller is identical to the order of the sliding mode that it is aimed at enforcing.

Now, a suitable sliding function  $\sigma(I_t, V, \theta)$  for system (6) will be introduced, which permits to prove the achievement of Objective 1. The sliding function  $\sigma : \mathbb{R}^{3n} \rightarrow \mathbb{R}^n$  is given by

$$\sigma(I_t, V, \theta) = M_1 I_t + M_2 (V - V^*) - M_3 \theta, \quad (9)$$

where  $M_1, M_2$  and  $M_3$  are positive definite diagonal matrices (e.g.,  $M_1 = \text{diag}\{m_{1_1}, \dots, m_{1_n}\}$ ) suitable selected in order to assign the dynamics of system (3) on the manifold  $\sigma = \mathbf{0}$ . Since  $M_1, M_2, M_3$  are diagonal matrices,  $\sigma_i, i \in \mathcal{V}$ , depends only on the state variables locally available at the  $i$ -th node, facilitating the design of a decentralized control scheme (see Remark 2). By regarding the sliding function (9) as the output function of system (3), it appears that the relative degree<sup>¶</sup> of the system is one. This implies that a first order SM controller can be *naturally* applied [19] in order to attain in a finite time the sliding manifold  $\sigma = \mathbf{0}$ . In this case, the discontinuous control signal generated by a first order SM controller can be directly used to open and close the switch of the boost converter.

**Remark 4 (Duty cycle)** *By using a discontinuous SM control law to open and close the switch of the boost converter, the Insulated Gate Bipolar Transistors (IGBTs) switching frequency cannot be a-priori fixed and the corresponding power losses could be very high. Usually, in order to achieve a constant IGBTs switching frequency, boost converters are controlled by implementing the so-called Pulse Width Modulation (PWM) technique. To do this, a continuous control signal that represents the so-called duty cycle of the boost converter is required.*

In order to obtain a continuous control signal, the procedure suggested in [23] is adopted, yielding for system (6)

$$\begin{aligned} L_t \dot{I}_t &= -R_t I_t - u \circ V + V_{DC} \\ C_t \dot{V} &= u \circ I_t - \mathcal{B} R^{-1} \mathcal{B}^T V - I_L \\ \dot{\theta} &= -(V - V^*) \\ \dot{u} &= h, \end{aligned} \quad (10)$$

where  $h \in \mathbb{R}^n$  is the new (discontinuous) SM control input. From (10) one can observe that the system relative degree (with respect to  $h$ ) is two. Then, it is possible to rely on a second order SM control strategy in order to steer the state of system (10) to the sliding manifold  $\sigma = \dot{\sigma} = \mathbf{0}$  for all  $t \geq T_r$ . Now, a specific second order SM controller is discussed, namely, the well known Suboptimal SOSM (SSOSM) controller proposed in [23]. Define  $d_i$  equal to  $\sum_{j \in \mathcal{N}_i} I_{ij}$ , with  $I_{ij}$  given by (2). For each node two auxiliary

<sup>¶</sup>The relative degree is the minimum order  $\rho$  of the time derivative  $\sigma_i^{(\rho)}, i \in \mathcal{V}$ , of the sliding function associated to the  $i$ -th node in which the control  $u_i, i \in \mathcal{V}$ , explicitly appears.



Fig. 2. Photo of the RSE's DC microgrid adopted during the test.

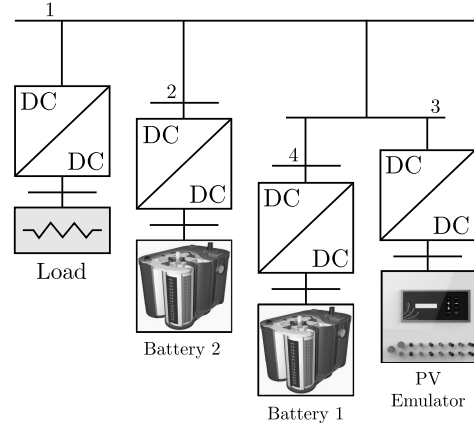


Fig. 3. Layout of the RSE's DC microgrid adopted during the test.

variables are defined,  $\xi_{1i} = \sigma_i$ ,  $\xi_{2i} = \dot{\sigma}_i$ ,  $i \in \mathcal{V}$ , and the so-called auxiliary system is build as follows:

$$\begin{aligned} \dot{\xi}_{1i} &= \xi_{2i} \\ \dot{\xi}_{2i} &= \phi_i(\dot{I}_{ti}, \dot{V}_i, \dot{d}_i, u_i) - \gamma_i(I_{ti}, V_i)h_i \\ \dot{u}_i &= h_i, \end{aligned} \quad (11)$$

where  $\xi_{2i}$  is not measurable since  $I_{L_i}$  is unknown and the parameters of the model are uncertain. Bearing in mind that  $\xi_{2i} = \dot{\sigma}_i = \phi_i + \gamma_i h_i$ , the expressions for  $\phi_i$  and  $\gamma_i$  are straightforwardly obtained from (9) by taking the second time derivative of  $\sigma_i$ . The following assumption is made on  $\phi_i$  and  $\gamma_i$ ,  $i \in \mathcal{V}$ :

**Assumption 3 (Bounded uncertainty)**  $\phi_i$  and  $\gamma_i$  in (11) have known bounds, i.e.,

$$|\phi_i(\cdot)| \leq \Phi_i \quad \forall i \in \mathcal{V} \quad (12)$$

$$0 < \Gamma_{\min_i} \leq \gamma_i(\cdot) \leq \Gamma_{\max_i}, \quad \forall i \in \mathcal{V}, \quad (13)$$

$\Phi_i$ ,  $\Gamma_{\min_i}$  and  $\Gamma_{\max_i}$  being positive constants.

**Remark 5 (Unknown bounds)** Note that in practical cases the bounds in (12) and (13) can be determined relying on data analysis and physical insights. However, if these bounds cannot be a-priori estimated, the Adaptive SSOSM algorithm [24] can be used to dominate the uncertainty.

With reference to [23], for each DGU  $i \in \mathcal{V}$ , the control law that is proposed to steer  $\xi_{1i}$ ,  $\xi_{2i}$  to zero in a finite time can be expressed as

$$h_i = \alpha_i H_{\max_i} \operatorname{sgn} \left( \xi_{1i} - \frac{1}{2} \xi_{1, \max_i} \right), \quad (14)$$

with

$$H_{\max_i} > \max \left( \frac{\Phi_i}{\alpha_i^* \Gamma_{\min_i}}; \frac{4\Phi_i}{3\Gamma_{\min_i} - \alpha_i^* \Gamma_{\max_i}} \right), \quad (15)$$

$$\alpha_i^* \in (0, 1] \cap \left( 0, \frac{3\Gamma_{\min_i}}{\Gamma_{\max_i}} \right), \quad (16)$$

$\alpha_i$  switching between  $\alpha_i^*$  and 1, according to [23, Algorithm 1]. Note that the control input  $u_i(t) = \int_0^t h_i(\tau) d\tau$ , is

continuous. Then,  $\delta_i = 1 - u_i$  can be used as duty cycle of the  $i$ -th boost converter. Note also that the design of the local controller for each DGU is not based on the knowledge of the whole microgrid, making the control synthesis simpler and the proposed control scheme scalable. We refer to [25] for the stability analysis of the controlled systems, but the main result is stated here for the sake of exposition.

**Theorem 1 (Local exponential stability).** Let Assumptions 1-3 hold. The desired operating point  $(\bar{I}_t, V^*, \theta)$  of system (6) can be made locally exponentially stable on the sliding manifold characterized by  $\sigma = \dot{\sigma} = 0$ , by choosing the entries of  $M_2$  sufficiently large.

## V. EXPERIMENTAL RESULTS

In order to verify the proposed control strategy, experimental tests are carried out using the DC microgrid test facility at RSE, shown in Figs. 2 and 3. The RSE's DC grid is unipolar with a nominal voltage of 380 V, including a resistive load (Node 1) with a maximum power of 30 kW at 400 V, a DC generator (Node 3) with a maximum power of 30 kW (used as PV emulator) and two energy storage systems (Node 2 and Node 4), based on high temperature NaNiCl batteries, each of them with an energy of 18 kWh and a maximum power of 30 kW for 10 s. These components

TABLE II  
RSE DC MICROGRID PARAMETERS

Symbol	Value	Unit	Description
$V_i^*$	380	V	DC nominal voltage
$V_{DC_i}$	$\approx 270$	V	DC input voltage
$R_{12}$	125	m $\Omega$	Tie-Line resistance 1-2
$R_{13}$	19.5	m $\Omega$	Tie-Line resistance 1-3
$R_{34}$	125	m $\Omega$	Tie-Line resistance 3-4
$L_{12}$	70	$\mu$ H	Tie-Line inductance 1-2
$L_{13}$	43	$\mu$ H	Tie-Line inductance 1-3
$L_{34}$	70	$\mu$ H	Tie-Line inductance 3-4
$C_{ti}$	6.8	mF	Output capacitance
$L_{ti}$	1.12	mH	Input inductance
$f_{sw}$	4	kHz	Switching frequency

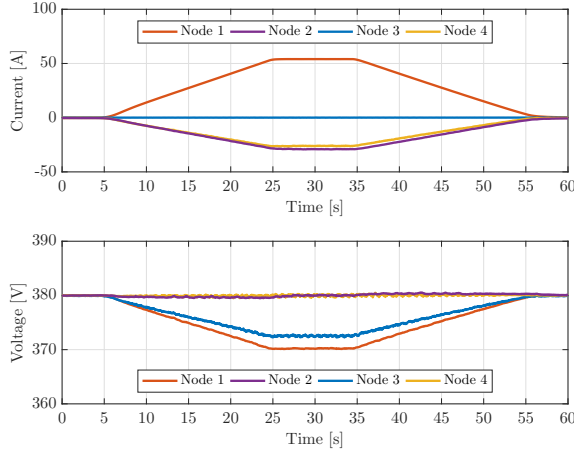


Fig. 4. Scenario 1: system performance with a load variation of about 20 kW in case of ramp rate equal to 1 kW/s.

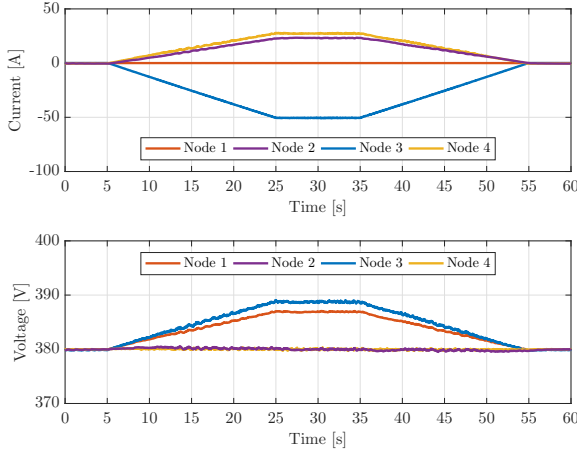


Fig. 5. Scenario 1: system performance with a generator variation of about 20 kW in case of ramp rate equal to 1 kW/s.

are connected to a common DC link through four DC-DC boost synchronous converters of 35 kW. The DC-DC converters are distributed and connected to the DC link with power distribution lines, the parameters of which are reported in Table II. The control of each converter is realized through two dSpace controllers that measure the inductor current and the boost output voltage and drive the power electronic converters. The DC-DC load and generator converters are controlled in constant power mode and are treated as current disturbances. The battery converters are controlled through the proposed SSOSM control scheme described in Section IV, where the voltage reference is set equal to 380 V. For both the battery converters, the SSOSM control parameters are  $m_{1_i} = 0.01$ ,  $m_{2_i} = 0.1$ ,  $m_{3_i} = 1$ ,  $H_{\max_i} = 4$ , and  $\alpha_i^* = 0.05$ . In order to test the performance of the proposed control approach, three different scenarios are implemented. Note that in the following figures we arbitrarily assume that the current entering any node is positive (passive sign convention).

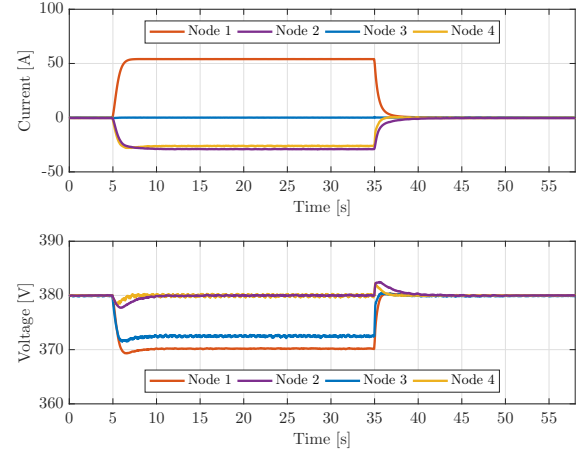


Fig. 6. Scenario 2: system performance with a step load variation of about 20 kW.

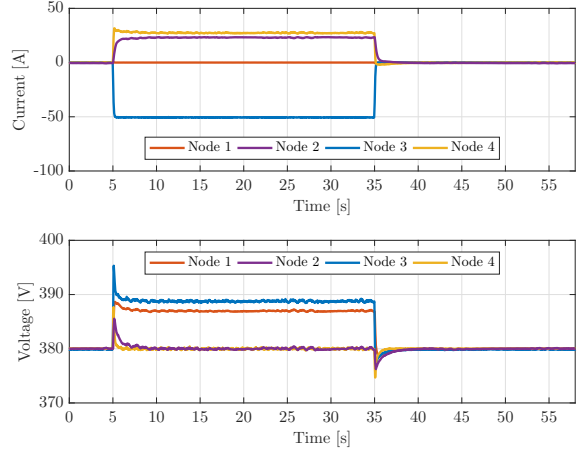


Fig. 7. Scenario 2: system performance with a step generator variation of about 20 kW.

**Scenario 1. Disturbance with a limited ramp rate power variation:** We assume that the system is in a steady state condition with zero power absorbed by the load or provided by the generator. At the time instant  $t = 5$  s the power reference for the load converter (see Fig. 4) or for the generator converter (see Fig. 5) is set to 20 kW and at the time instant  $t = 35$  s is reset to 0 kW with the ramp rate limited to 1 kW/s. The proposed control strategy is able to keep the output voltage of both the batteries DC-DC converter to their reference without any voltage variation.

**Scenario 2. Disturbance with a step power variation:** The tests in Scenario 1 are replicated without ramp rate limitation. In this case, due to the step power variation, one can observe a voltage transient, after which the system exhibits a stable performance thanks to the robustness of the proposed control approach (see Figs. 6 and 7).

**Scenario 3. Step variation of the voltage reference:** In this scenario the proposed primary controllers have been coupled with a secondary control scheme that calculates the voltage references for the battery converters in order

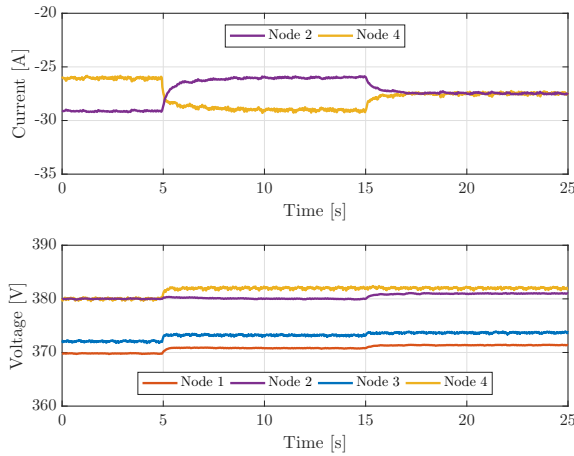


Fig. 8. Scenario 3: system performance in case of constant load (20 kW) and voltage reference variation for the DC-DC battery converters in order to obtain current sharing.

to achieve current sharing among the batteries (see Fig. 8). Although the analysis of a secondary control level is not discussed in this paper, Scenario 3 is aimed at showing that the proposed primary controllers, due to their robustness property in tracking the voltage references, can be coupled with any secondary control scheme that guarantees current or power sharing.

Finally, note that in the discussed scenarios, only the voltage of the battery nodes (Node 2 and Node 4) have been controlled with the proposed strategy. Nevertheless, the voltage deviations from the nominal value in the other two nodes (Node 1 and Node 3), depending on the line impedances, are always less than 3%.

## VI. CONCLUSIONS

In this paper a robust control strategy has been designed to regulate the voltage in boost-based DC microgrids. The proposed control scheme is fully decentralized and is based on higher order sliding mode control methodology, which allows to obtain continuous control inputs. The latter can be used as duty cycles of the boost converters, achieving constant switching frequency and facilitating a PWM-based implementation. The proposed control scheme has been validated through experimental tests on a real DC microgrid, showing satisfactory closed-loop performances.

## REFERENCES

- [1] J. M. Guerrero, F. Blaabjerg, T. Zhelev, K. Hemmes, E. Monmasson, S. Jemei, M. P. Comech, R. Granadino, and J. I. Frau, "Distributed generation: Toward a new energy paradigm," *IEEE Industrial Electronics Magazine*, vol. 4, no. 1, pp. 52–64, Mar. 2010.
- [2] N. L. Panwar, S. C. Kaushik, and S. Kothari, "Role of renewable energy sources in environmental protection: A review," *Renewable and Sustainable Energy Reviews*, vol. 15, no. 3, pp. 1513 – 1524, 2011.
- [3] M. Liserre, T. Sauter, and J. Y. Hung, "Future energy systems: Integrating renewable energy sources into the smart power grid through industrial electronics," *IEEE Industrial Electronics Magazine*, vol. 4, no. 1, pp. 18–37, Mar. 2010.

- [4] R. Lasseter and P. Paigi, "Microgrid: a conceptual solution," in *Proc. 35th IEEE Power Electron. Specialists Conf.*, vol. 6, Aachen, Germany, Jun. 2004, pp. 4285–4290.
- [5] M. S. Sadabadi, Q. Shafiee, and A. Karimi, "Plug-and-play voltage stabilization in inverter-interfaced microgrids via a robust control strategy," *IEEE Transactions on Control Systems Technology*, vol. 25, no. 3, pp. 781–791, May 2017.
- [6] S. Trip, M. Bürger, and C. De Persis, "An internal model approach to frequency regulation in inverter-based microgrids with time-varying voltages," in *Proc. of the 53rd IEEE Conference on Decision and Control (CDC)*, Dec. 2014, pp. 223–228.
- [7] M. Cucuzzella, G. P. Incremona, and A. Ferrara, "Decentralized sliding mode control of islanded ac microgrids with arbitrary topology," *IEEE Transactions on Industrial Electronics*, Apr. 2017.
- [8] C. De Persis and N. Monshizadeh, "Bregman storage functions for microgrid control," *IEEE Transactions on Automatic Control*, vol. PP, no. 99, pp. 1–1, 2017.
- [9] J. W. Simpson-Porco, F. Dörfler, and F. Bullo, "Synchronization and power sharing for droop-controlled inverters in islanded microgrids," *Automatica*, vol. 49, no. 9, pp. 2603–2611, 2013.
- [10] J. Schiffer, R. Ortega, A. Astolfi, J. Raisch, and T. Sezi, "Conditions for stability of droop-controlled inverter-based microgrids," *Automatica*, vol. 50, no. 10, pp. 2457–2469, 2014.
- [11] J. J. Justo, F. Mwasilu, J. Lee, and J.-W. Jung, "AC-microgrids versus DC-microgrids with distributed energy resources: A review," *Renewable Sustain. Energy Rev.*, vol. 24, pp. 387–405, Aug. 2013.
- [12] S. Anand, B. G. Fernandes, and J. Guerrero, "Distributed control to ensure proportional load sharing and improve voltage regulation in low-voltage DC microgrids," *IEEE Transactions on Power Electronics*, vol. 28, no. 4, pp. 1900–1913, Apr. 2013.
- [13] J. Zhao and F. Dörfler, "Distributed control and optimization in DC microgrids," *Automatica*, vol. 61, pp. 18 – 26, Nov. 2015.
- [14] S. Trip, M. Cucuzzella, C. De Persis, X. Cheng, and A. Ferrara, "Sliding modes for voltage regulation and current sharing in dc microgrids," in *Proc. American Control Conference*, Milwaukee, WI, USA, 2018.
- [15] V. Nasirian, S. Moayedi, A. Davoudi, and F. L. Lewis, "Distributed cooperative control of DC microgrids," *IEEE Transactions on Power Electronics*, vol. 30, no. 4, pp. 2288–2303, Apr. 2015.
- [16] M. Tucci, L. Meng, J. M. Guerrero, and G. Ferrari Trecate, "Consensus algorithms and plug-and-play control for current sharing in DC microgrids," *arXiv preprint arXiv:1603.03624*, Mar. 2017.
- [17] C. De Persis, E. R. Weitenberg, and F. Dörfler, "A power consensus algorithm for dc microgrids," *Automatica*, vol. 89, pp. 364–375, 2018.
- [18] R. Han, M. Tucci, R. Soloperto, A. Martinelli, G. Ferrari-Trecate, and J. M. Guerrero, "Hierarchical plug-and-play voltage/current controller of dc microgrid with grid-forming/feeding converters: Line-independent primary stabilization and leader-based distributed secondary regulation," *arXiv preprint arXiv:1707.07259*, 2017.
- [19] V. Utkin, *Sliding Modes in Control and Optimization*, ser. Communication and control engineering. Springer-Verlag, 1992.
- [20] D. Ronchegalli and R. Lazzari, "Development of the control strategy for a direct current microgrid: A case study," in *2016 AEIT International Annual Conference (AEIT)*, Oct 2016, pp. 1–6.
- [21] H. Akagi, E. H. Watanabe, and M. Aredes, *Instantaneous power theory and applications to power conditioning*. John Wiley & Sons, 2007, vol. 31.
- [22] F. Dörfler and F. Bullo, "Kron reduction of graphs with applications to electrical networks," *IEEE Transactions on Circuits and Systems I: Regular Papers*, vol. 60, no. 1, pp. 150–163, Jan 2013.
- [23] G. Bartolini, A. Ferrara, and E. Usai, "Chattering avoidance by second-order sliding mode control," *IEEE Transactions on Automatic Control*, vol. 43, no. 2, pp. 241–246, Feb. 1998.
- [24] G. P. Incremona, M. Cucuzzella, and A. Ferrara, "Adaptive suboptimal second-order sliding mode control for microgrids," *Int. J. Control*, vol. 89, no. 9, pp. 1849–1867, Jan. 2016.
- [25] M. Cucuzzella, R. Lazzari, S. Trip, S. Rosti, C. Sandroni, and A. Ferrara, "Sliding mode voltage control of boost converters in DC microgrids," *Control Engineering Practice*, vol. 73, pp. 161–170, 2018.